

PAPER • OPEN ACCESS

Effect of shape and thickness of asbestos bundles and fibres on EDS microanalysis: A Monte Carlo simulation

To cite this article: D Moro and G Valdre 2016 *IOP Conf. Ser.: Mater. Sci. Eng.* **109** 012011

View the [article online](#) for updates and enhancements.

Related content

- [Low voltage imaging and X-ray microanalysis in the SEM: challenges and opportunities](#)

R Wuhrer and K Moran

- [Low voltage EPMA: experiments on a new frontier in microanalysis - analytical lateral resolution](#)

J Fournelle, H Cathey, P T Pinard et al.

- [Electron probe microanalysis of Ni-silicides at low voltage: difficulties and possibilities](#)

E. Heikinheimo, P.T. Pinard, S. Richter et al.

Recent citations

- [Ceramic Recipes: Cross-correlated analytical strategy for the characterization of the Iron Age pottery from ancient Karkemish \(Turkey\)](#)

Gabriele Giacosa et al



IOP | ebooks™

Bringing you innovative digital publishing with leading voices to create your essential collection of books in STEM research.

Start exploring the collection - download the first chapter of every title for free.

Effect of shape and thickness of asbestos bundles and fibres on EDS microanalysis: a Monte Carlo simulation

D Moro and G Valdrè

University of Bologna, Interdisciplinary Research Centre of Biomineralogy, Cristallography and Biomaterials, Department of Biological, Geological and Environmental Sciences, Geological Section, Piazza di Porta San Donato 1, 40126 Bologna, Italy

E-mail: giovanni.valdre@unibo.it

Abstract. Quantitative microanalysis of tiny asbestos mineral fibres by scanning electron microscopy equipped with energy-dispersive X-ray spectroscopy (SEM-EDS) still represents a complex analytical issue. This complexity arises from the variable fibre shape and small thickness ($< 5 \mu\text{m}$) compared with the penetration of the incident electron beam. Here, we present the results of Monte Carlo simulations of chrysotile, crocidolite and amosite fibres (and bundles of fibres) of circular and square section and thicknesses from $0.1 \mu\text{m}$ to $10 \mu\text{m}$, to investigate the effect of shape and thickness on SEM-EDS microanalysis. The influence of shape and thickness on the simulated spectrum was investigated for electron beam energies of 5, 15 and 25 keV, respectively. A strong influence of the asbestos bundles and fibres shape and thickness on the detected EDS X-ray intensity was observed. The X-ray intensity trends as a function of fibre thickness showed a non-linear dependence for all the elements and minerals. In general, the X-ray intensities showed a considerable reduction for thicknesses below about $0.5 \mu\text{m}$ at 5 keV, $2 \mu\text{m}$ at 15 keV, and $5 \mu\text{m}$ at 25 keV. Correction parameters, k -ratios, for the asbestos fibre thickness effect, are reported.

1. Introduction

Precise chemical analysis of asbestos fibres is important for their identification and in depth mineral characterisation. Fibres composition is also an important criteria in understanding the minerals' environmental and health impacts, and determining the potential to have toxicological effects [1-3].

In vitro and *in vivo* studies revealed that asbestos fibres toxicity is strongly related to the chemical composition, particularly as regards the Fe content and its oxidation state [4]. In addition, asbestos-induced cytotoxicity and genotoxicity is thought to be also due to the generation of reactive oxygen species and other radicals that are catalysed by iron ions at the fibre surface [5]. A strong biochemical reaction is induced in biological systems by the mineral composition of fibres with bonded metal ions. Fundamental cell biology research on the interaction of cells with long fibres or fibres containing highly reactive chemical species will be facilitated by techniques able to accurately quantify the chemistry of mineral fibres *in situ* [6].

Scanning electron microscopy equipped with X-ray energy dispersive spectroscopy (SEM-EDS) is of great importance for minerals, materials and biomaterials characterisation, and in evaluating the phenomena and possible mechanism of interaction between materials and bio-entities [7-9].

Energy-dispersive X-ray spectroscopy (EDS) is by far the most routine method for asbestos chemical analysis [1]. However, SEM-EDS quantitative microanalysis of asbestos mineral fibres may



Content from this work may be used under the terms of the [Creative Commons Attribution 3.0 licence](#). Any further distribution of this work must maintain attribution to the author(s) and the title of the work, journal citation and DOI.

suffer from systematic errors because of the variable fibre shape and small thickness ($< 5 \mu\text{m}$) compared with the penetration of the incident electron beam. In the classical correction methods used in quantitative microanalysis of bulk samples for the correction of matrix effects, e.g., ZAF or $\phi(\rho z)$ procedures, both standard and sample are assumed to have flat polished surfaces and be infinitely thick with respect to the penetration of the electron beam.

In the case of micro- and sub-micrometric particles their size and shape may cause large errors in the quantification due to particle effects on the generation and measurement of X-rays from the sample. These ones are related to the elastic scattering of electrons in the finite size (mass) of the fibre, strongly influenced by the average atomic number. For a given mean atomic number, the thickness of the particle is key, with a shape component affecting the absorption and fluorescence contributions to the correction routine. In the analysis of micro- and sub-micrometric particles, X-ray emergence angle and absorption path length cannot be determined as for flat polished samples [10, 11]. Furthermore we point out that EDS systems, because they are often set to normalize the results, are prone to hide poor analytical results, like high or low totals, which then hide any problem in the analytical protocol.

The empirical methods proposed to overcome these issues are, however, cumbersome and need characterized standards for thickness, geometry and composition [11, 12].

The Monte Carlo method is a valuable tool for investigating the basis, the reliability and the limitations of quantification procedures. In particular, Monte Carlo simulations can be of paramount importance for studying the electron transport and X-ray generation in samples with complex geometry or under unconventional measurement conditions [13-15].

Here, we report the results of Monte Carlo simulations of asbestos fibres and bundles of fibres to investigate the effect of shape and thickness on SEM-EDS microanalysis. NISTMONTE [16] was used to simulate electron transport, X-ray generation and detection in complex sample geometries. The investigated asbestos minerals were chrysotile, amosite and crocidolite.

Chrysotile, white asbestos, is a phyllosilicate of the serpentine group. About 95% of asbestos used in commercial products was chrysotile [17, 18].

Crocidolite, blue asbestos, and amosite, brown asbestos, are members of the amphiboles group and are the most commonly used amphibole asbestos. The term crocidolite is used for the asbestos variety of the amphibole mineral riebeckite, whereas amosite for the asbestos variety of grunerite, as indicated by Gunter and co-workers [1]. They contain high levels of iron as a normal constituent of the crystal structure. Amphibole exposure is greater than chrysotile in the natural environment, since amphiboles are more widespread than chrysotile [1, 17, 19-21].

2. Methods and simulation models

2.1. Methods

The Monte Carlo simulations were carried out using the programme NISTMONTE version 2 [16], which simulates electron transport, X-ray generation and transmission in complex sample geometries. Monte Carlo method applied to electron and X-ray transport is used to simulate electrons trajectories and X-rays through the mineral fibre and to the X-ray detector. Accurate quantitative analysis by X-ray spectroscopy requires the understanding of electron scattering, X-ray generation, absorption and fluorescence.

NISTMONTE 2 implements a single scattering model to track electrons trajectories as they interact with matter. It uses three different elastic scattering models: a basic screened Rutherford model, the Mott scattering cross-section of Czyzewski and co-workers [22], and the Mott cross-section of Jablonski and co-workers [23]. The energy loss is modelled using the Joy-Luo expression [24], which is an empirical modification of the Bethe energy loss equation [25]. The ionisation cross-section is modelled using the empirical expression of Casnati [26]. The mass absorption coefficients are those of Heinrich [27], and the fluorescence yields are tabulated experimental values [28].

The electron source is defined to be a Gaussian beam. The emitted x-ray events are convolved with a response function that mimics the energy resolution of an EDS detector. The simulated EDS spectra

of single asbestos and bundles of fibres were used to evaluate the effect of shape and thickness by integrating and comparing peaks intensity as a function of thickness, shape and beam energy for each mineral, after background subtraction.

2.2. Simulation models

Bundles and fibres of variable shape and thickness on a pure carbon holder were simulated taking into account realistic experimental conditions, such as sample geometry, SEM set-up and detector physics.

We investigated chrysotile, crocidolite and amosite with chemical formulae as specified in Table 1.

Table 1. Chemical formulae of the simulated asbestos.

Mineral name	Chemical formulae
Chrysotile	$Mg_3Si_2O_5(OH)_4$
Crocidolite	$NaFe^{2+}_{2.25}Mg_{0.25}Fe^{3+}_2Si_8O_{22}(OH)_2$
Amosite	$Fe^{2+}_{5.25}Mg_{1.75}Si_8O_{22}(OH)_2$

Two models for each mineral were taken into account: (i) a three-dimensional fibre of circular section, 100 µm long and with thicknesses ranging from to 0.1 µm to 5 µm, deposited on a flat graphite support, and (ii) a three-dimensional bundle of square section, 100 µm long and with thicknesses ranging from to 0.1 µm to 10 µm, deposited on a flat graphite support.

An electron probe of 40 nm in diameter focussed in parallel illumination onto the surface of the fibre or bundle, in a mid position with respect to the edges, was taken into account. The modelled EDS detector used to generate the spectrum had a gold layer of 7 nm, a dead layer of 10 nm, a detector diode thickness of 3 mm, solid angle of $5 \cdot 10^{-3}/4\pi$, 4,096 channels each of 10 eV and a resolution of 130 eV (at Mn K α). The detector elevation angle was set to 40°, with an azimuthal angle of 0°. The fibre or bundle was oriented with its long axis in the same direction as the detector.

The influence of shape and thickness on the simulated spectrum was investigated for electron beam energies of 5, 15 and 25 keV.

3. Results and discussion

In conventional SEM-EDS microanalysis (with beam energy 10 - 30 keV) the sizes of the electron beam interaction volume and X-ray generation volume are on the order of micrometres in most materials. When particle size is smaller than the primary electron beam penetration depth, a portion of the beam escapes the particle before exciting X-rays (finite size effect). Thus, a fraction of the electron beam scatters out of the particle volume and can excite X-rays from the substrate or adjacent particles. These phenomena can affect the analytical results.

Figure 1 shows, as an example, a section image of the simulated trajectories of electrons for a 25 keV electron beam focussed onto the surface of a chrysotile circular fibre, in a mid position with respect to the edges. The fibre has a diameter of 2 µm and is deposited on a graphite substrate. The primary electrons (green vertical beam) interact with the fibre as visualized by the fuchsia trajectories. At this energy level a fraction of the electrons penetrate into the graphite substrate (grey trajectories) for several micrometres. Furthermore, a fraction of the electrons scatters out of the fibre volume from its sides, both toward the substrate, green trajectories, and leaving the fibre and the substrate, blue lines.

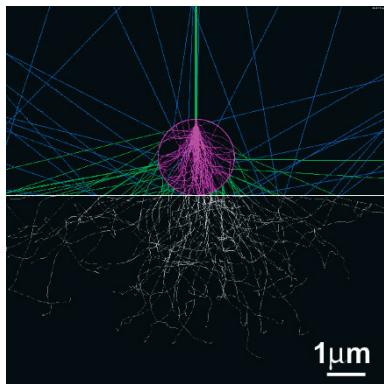


Figure 1. Simulated trajectory of electrons as they interact with the sample (chrysotile) and the substrate (graphite). 2D view of the 3D simulated trajectory of electrons (fuchsia: interacting with the sample; green and grey: towards and penetrating the substrate, respectively; blue: exiting) as they interact with a chrysotile cylindrical fibre (marked with a fuchsia circular line) deposited on a bulk graphite substrate (marked with a grey horizontal line). The view is from the direction parallel to the long axis of the cylindrical fibre.

To help the reader in the analysis of the results we report in Table 2 the nominal range value (for a bulk sample) of electron penetration depth, and X-rays intensity (generated and emitted) for the three mineral samples and the three beam energies considered in this work. The calculation was performed with the same SEM set-up reported in Section 2.2 considering 1,000 electron trajectories. The table report the absolute magnitude of generated and emitted X-ray intensity for each X-ray line calculated on bulk samples, in arbitrary units as reported by Ritchie [29].

Table 2. Electron penetration depth (e.p.d., in μm) and absolute magnitude (arbitrary units) of generated (g) and emitted (e) X-ray intensity for each X-ray line calculated on bulk samples (as reported by Ritchie [29]).

	Chrysotile			Crocidolite			Amosite		
	5keV	15keV	25keV	5keV	15keV	25keV	5keV	15keV	25keV
e.p.d. [μm]	0.38	2.20	5.09	0.26	1.76	4.12	0.27	1.47	3.76
Na K _α	—	—	—	(g) 7.0 (e) 5.9	(g) 38 (e) 14	(g) 74 (e) 11	—	—	—
Fe K _α	—	—	—	0 (e) 21	(g) 21 (e) 78	(g) 81	0 (e) 24	(g) 24 (e) 93	(g) 97
Fe K _β	—	—	—	0 (e) 2.5	(g) 2.6 (e) 10	(g) 10	0 (e) 3.0	(g) 3.0 (e) 12	(g) 12
Fe L	—	—	—	(g) 29 (e) 27	(g) 130 (e) 30	(g) 240 (e) 20	(g) 34 (e) 26	(g) 150 (e) 40	(g) 290 (e) 30
Mg K _α	(g) 27 (e) 26	(g) 170 (e) 110	(g) 340 (e) 130	(g) 2.2 (e) 2.0	(g) 14 (e) 7	(g) 27 (e) 6	(g) 5.0 (e) 4.5	(g) 30 (e) 15	(g) 61 (e) 15
Si K _α	(g) 12 (e) 12	(g) 100 (e) 70	(g) 220 (e) 100	(g) 16 (e) 15	(g) 140 (e) 100	(g) 280 (e) 130	(g) 16 (e) 15	(g) 130 (e) 90	(g) 270 (e) 130
O K _α	(g) 130 (e) 120	(g) 550 (e) 220	(g) 1,000 (e) 170	(g) 120 (e) 100	(g) 470 (e) 190	(g) 860 (e) 150	(g) 110 (e) 100	(g) 440 (e) 180	(g) 820 (e) 150

3.1. Chrysotile

To investigate the significance of the thickness and shape effects on chrysotile, a fibre of circular section and a bundle of square section were taken into account with a composition as reported in Table 1. See section 2.2 for details on the simulation model. Figure 2 shows the trend of the integrated intensities (counts), obtained from the simulated EDS spectra, as a function of thickness (fibre diameter or bundle thickness) for each element (Si, Mg, O) of the mineral at beam energies of 5 keV, 15 keV and 25 keV (see the legend in figure 2e). Figures 2a, 2c and 2e shows the simulation results of the circular fibre for thickness form 0.1 μm to 5 μm , whereas figures 2b, 2d and 2f those of the bundle of square section for thickness form 0.1 μm to 10 μm .

A strong dependence of the simulated X-ray intensity on the fibre thickness was observed for all the elements of both models. Note that the intensity values reported for thickness of 10 μm can be considered as a reference value valid for a massive sample. By comparing the intensity values for a 10 μm thick sample with those calculated for a bulk one, we verified that a thickness of 10 μm represents, at the simulated experimental conditions, a bulk sample for all minerals and energies here considered. We report in Table 3 the reference intensity values for bulk samples calculated at an electron beam energy of 25 keV. Generally speaking, the integrated intensities start to have a reduction for thickness below 5 μm . In particular, for all the considered elements, Si, Mg and O, and both fibre and bundle, the integrated intensities strongly decrease starting from thickness of 5 μm at 25 keV, 2 μm at 15 keV and 0.5 μm at 5 keV. Notably, the square section bundle model presents a more marked effect of intensity enhancement before the reduction starting point. In terms of the previously cited finite size and reduced absorption effects, for the bundle model the reduced absorption effect initially prevails on the finite size one, which in turn becomes predominant for smaller thicknesses.

Table 3. Reference intensity values for a bulk sample at 25 keV in our experimental set up (§ 2.2).

	Na _{Kα}	Fe _{Kα}	Fe _{Kβ}	Fe _L	Mg _{Kα}	Si _{Kα}	O _{Kα}
Chrysotile	—	—	—	—	1.78·10 ⁶	1.40·10 ⁶	1.32·10 ⁶
Crocidolite	1.43·10 ⁵	1.14·10 ⁶	1.42·10 ⁵	1.86·10 ⁵	8.54·10 ⁴	1.90·10 ⁶	1.12·10 ⁶
Amosite	—	1.36·10 ⁶	1.70·10 ⁵	2.25·10 ⁵	2.00·10 ⁵	1.80·10 ⁶	1.09·10 ⁶

3.2. Crocidolite

A fibre of circular section and a bundle of square section were simulated also for crocidolite, with a composition as reported in Table 1. See section 2.2 for details on the simulation model. Figure 3 shows the results for the circular section fibre. It reports the trend of the integrated intensities (counts), obtained from the simulated EDS spectra, as a function of fibre diameter for each element of the mineral at beam energies of 5 keV, 15 keV and 25 keV (see legend in figure 3g). Fibres with a diameter from 0.1 μm to 5 μm were simulated. Bundles with a thickness from 0.1 μm to 10 μm were also simulated (data not shown, but available on request).

A strong dependence of the simulated X-ray intensity on the fibre thickness was observed for all the elements of both the models. The intensity values calculated for thicknesses of 10 μm were found very close to those calculated for a massive sample. Table 3 reports the reference intensity values for bulk samples calculated at an electron beam energy of 25 keV. Generally speaking, the integrated intensities start to have a reduction for thickness below 5 μm , with the exception of the Fe L-line which starts decreasing from 2 μm in the case of square section bundle. In particular, for almost all the considered elements, Si, Mg, O, Na, Fe (K α), Fe (K β), Fe (L), and both fibre and bundle, the integrated intensities strongly decrease starting from thickness of 5 μm at 25 keV, 2 μm at 15 keV and 0.5 μm at 5 keV.

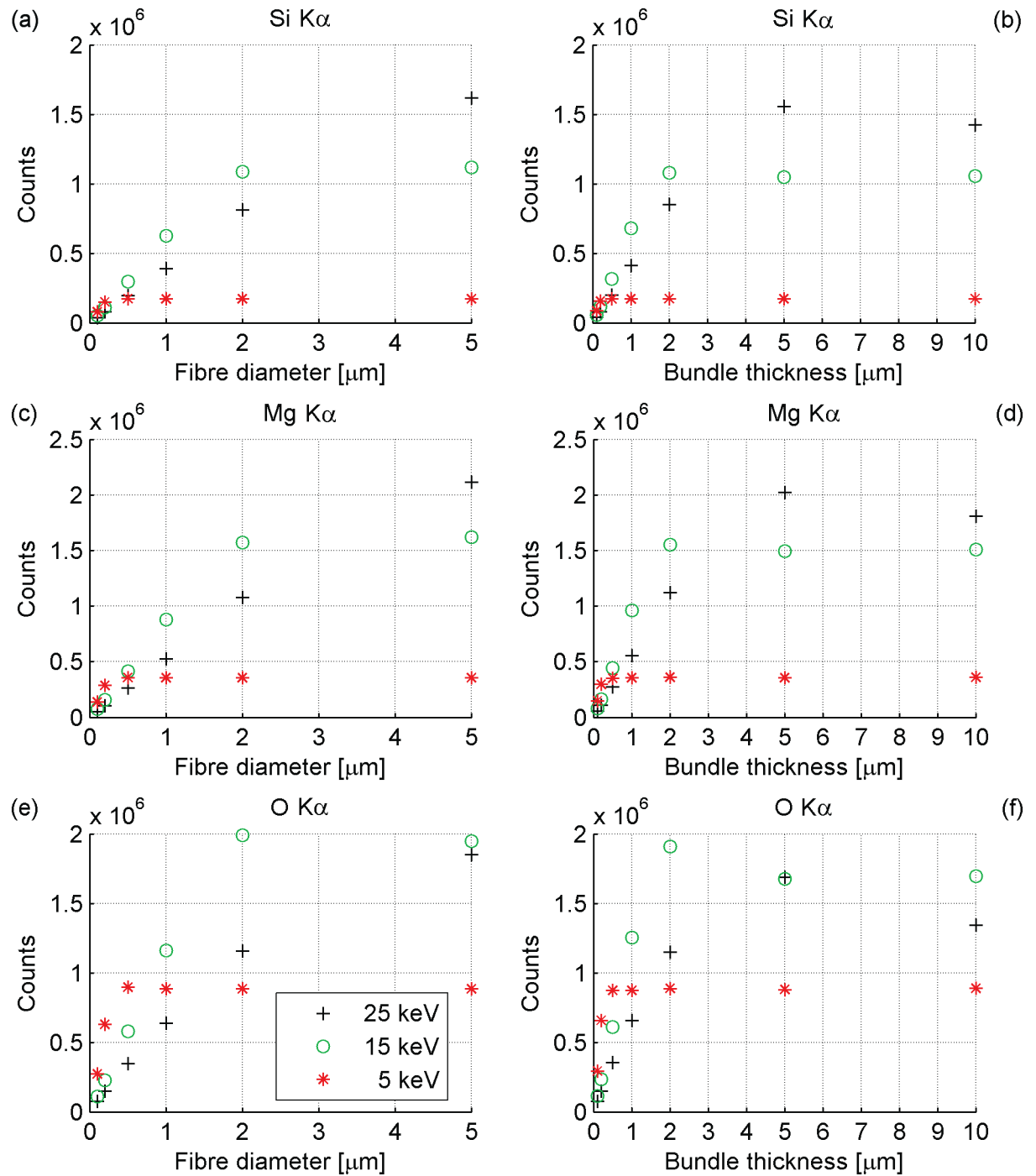


Figure 2. Simulated SEM-EDS K α -line X-ray intensity of Si, Mg and O as a function of thickness for a single chrysotile cylindrical fibre, (a), (c), (e), and for a bundle of fibres, (b), (d), (f), with beam energy of 5 keV, 15 keV and 25 keV; see legend in (e).

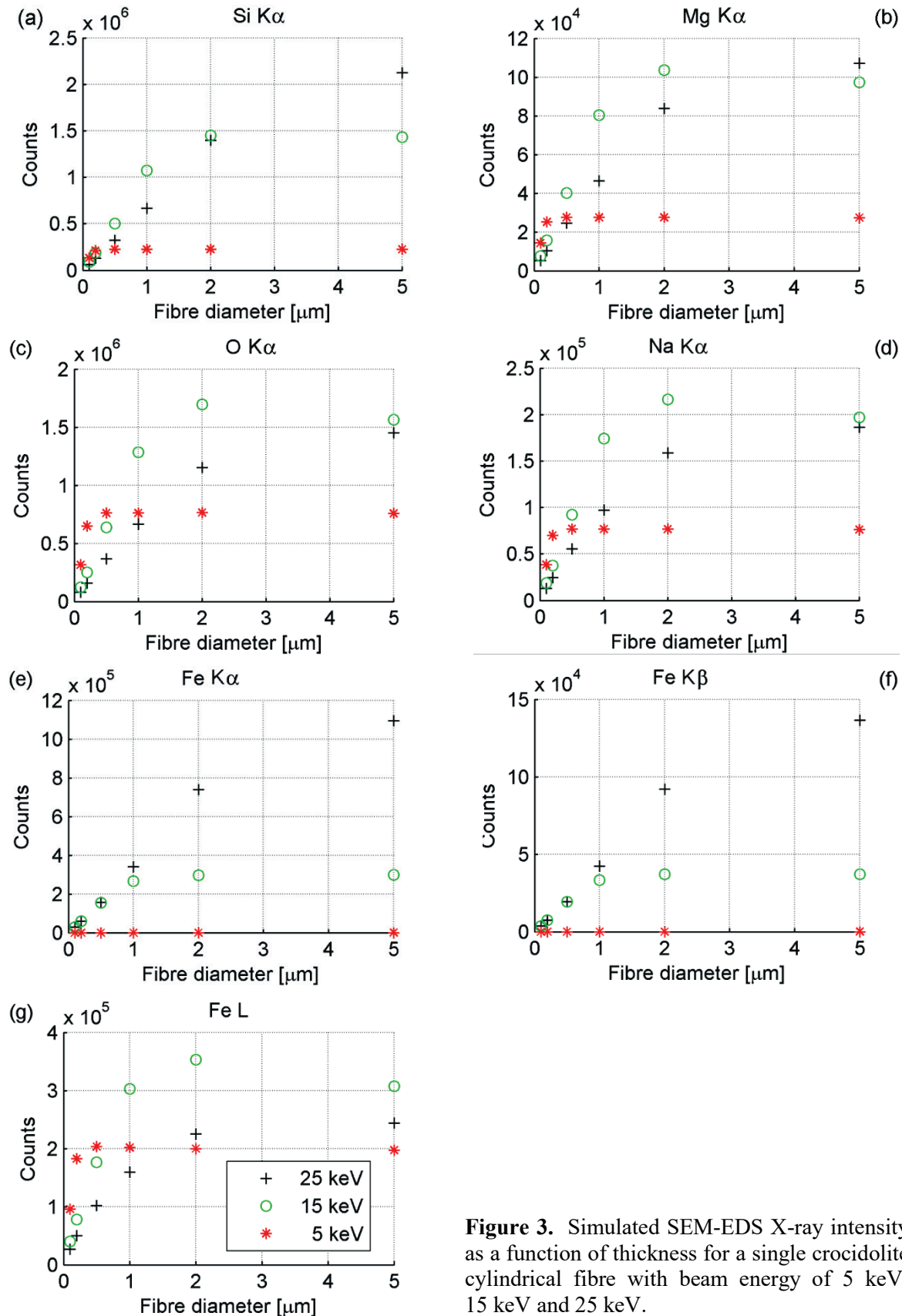


Figure 3. Simulated SEM-EDS X-ray intensity as a function of thickness for a single crocidolite cylindrical fibre with beam energy of 5 keV, 15 keV and 25 keV.

The two models present a similar effect of intensity enhancement before the reduction starting point. Again, in terms of the previously cited finite size and reduced absorption effects, the reduced absorption effect initially prevails on the finite size one, that in turn become predominant for smaller thicknesses. The magnitude of the reduced X-ray absorption effect is generally largest in the case for “soft” X-rays, when there is high absorption, in agreement with the experimental results of Paoletti and co-workers, and Small [10, 11].

3.3. Amosite

An amosite fibre of circular section and a bundle of square section were simulated, with a composition as reported in Table 1. See section 2.2 for details on the simulation model. Figure 4 shows the results for the circular section fibre. It reports the trend of the integrated intensities (counts), obtained from the simulated EDS spectra, as a function of fibre diameter for each element of the mineral at beam energies of 5 keV, 15 keV and 25 keV (see the legend in figure 4f). Fibres with a diameter from 0.1 μm to 5 μm were simulated. Bundles with a thickness from 0.1 μm to 10 μm were also simulated (data not reported, but available on request).

A strong dependence of the simulated X-ray intensity on the fibre thickness was observed for all the elements of both the models. The intensity values calculated for thicknesses of 10 μm were found very close to those calculated for a massive sample. Table 3 reports the reference intensity values for bulk samples calculated at an electron beam energy of 25 keV. Generally speaking, the integrated intensities start to have a reduction for thickness below 5 μm , with the exception of the Fe L-line which starts decreasing from 2 μm in the case of square section bundle. In particular, for almost all the considered elements, Si, Mg, O, Fe (K α), Fe (K β), Fe (L), and both fibre and bundle, the integrated intensities strongly decrease starting from thickness of 5 μm at 25 keV, 2 μm at 15 keV and 0.5 μm at 5 keV. The two models present a similar effect of intensity enhancement before the reduction starting point. Again, in terms of the previously cited finite size and reduced absorption effects, the reduced absorption effect initially prevails on the finite size one, that in turn becomes predominant for smaller thicknesses.

Our investigation may be used to develop specific thickness correction factors for SEM-EDS quantitative analysis. For the sake of example we report in Table 4 the k -ratios (intensity ratio of X-rays emitted by the mineral fibre to those produced by a massive sample) calculated for cylindrical fibres of different thickness at an electron beam energy of 15 keV.

4. Conclusions

A strong influence of the asbestos bundles and fibres thickness and shape on the detected EDS X-ray intensity was observed. In particular, the variation of the simulated X-ray intensity was significantly correlated with the mineral fibre thickness. The X-ray intensity trends as a function of thickness showed a non-linear dependence for all the elements and minerals. Generally speaking, the X-ray intensities showed a considerable reduction for thicknesses below about 0.5 μm at 5 keV, 2 μm at 15 keV, and 5 μm at 25 keV. Low voltages greatly reduce the excitation volume. Notably, an X-ray intensity enhancement was often observed before the reduction starting point, with a magnitude that depends on the mineral type, shape, specific element and beam energy. Monte Carlo simulation methods proved to be effective to face the thickness effects in SEM-EDS microanalysis with approaches that appear less complex and cumbersome than experimental ones.

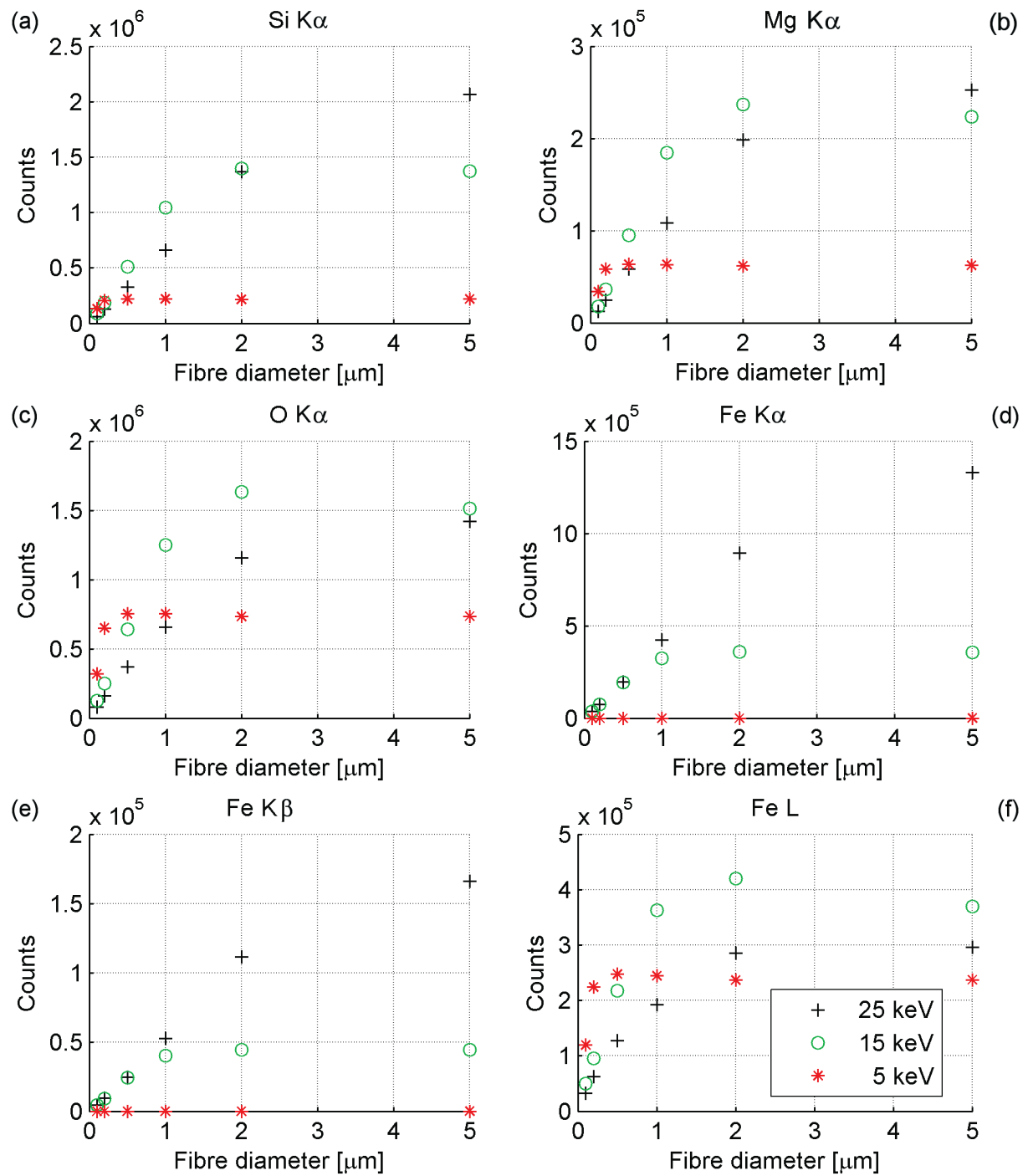


Figure 4. Simulated SEM-EDS X-ray intensity as a function of thickness for a single amosite cylindrical fibre with beam energy of 5 keV, 15 keV and 25 keV.

Table 4. *k*-ratios calculated at 15 keV for cylindrical fibres of different thickness.

Mineral	Thickness	X-ray lines					
		Na _{Kα}	Fe _{Kα}	Fe _{Kβ}	Fe _L	Mg _{Kα}	Si _{Kα}
Chrysotile	2.0 µm	—	—	—	—	1.04	1.03
	1.0 µm	—	—	—	—	0.58	0.59
	0.5 µm	—	—	—	—	0.28	0.28
	0.1 µm	—	—	—	—	0.05	0.05
Crocidolite	2.0 µm	1.20	0.99	0.99	1.29	1.14	1.04
	1.0 µm	0.97	0.88	0.88	1.10	0.88	0.77
	0.5 µm	0.51	0.51	0.51	0.64	0.44	0.36
	0.1 µm	0.10	0.10	0.10	0.15	0.08	0.06
Amosite	2.0 µm	—	1.00	1.00	1.31	1.16	1.06
	1.0 µm	—	0.91	0.90	1.13	0.91	0.79
	0.5 µm	—	0.54	0.54	0.68	0.46	0.39
	0.1 µm	—	0.10	0.10	0.16	0.09	0.07

References

- [1] Gunter M E, Belluso E and Mottana A 2007 Amphiboles: environmental and health concerns. in: *Amphiboles: Crystal Chemistry, Occurrence, and Health Issues (Reviews in Mineralogy & Geochemistry vol 67)* (Hawthorne F C, Oberti R, Della Ventura G and Mottana A; Eds.) (Chantilly, VA: Mineralogical Society of America) chapter 12 pp 453-516
- [2] Bernstein D M and Hoskin J A 2006 *Regul. Toxicol. Pharmacol.* **45** 252
- [3] Bernstein D M 2014 Serpentine and amphibole asbestos. in: *Inhalation Toxicology* (3rd edition) (Salem H and Katz S A; Eds.) (Boca Raton, FL: CRC Press) 295-326
- [4] Hardy J A and Aust A E 1995 *Chem. Rev.* **95** 97
- [5] Gazzano E, Turci F, Foresti E, Putzu M G, Aldieri E, Silvagno F, Lesci I G, Tomatis M, Riganti C, Romano C, Fubini B, Roveri N and Ghigo D 2007 *Chem. Res. Toxicol.* **20** 380
- [6] Yao S, Della Ventura G and Petibois C 2010 *Anal. Bioanal. Chem.* **397** 2079
- [7] Bocchi G and Valdrè G 1993 *J. Inorg. Biochem.* **49** 209
- [8] Borgia G C, Brown R J S, Fantazzini P, Mesini E and Valdrè G 1992 *Nuovo Cimento* **14** 745
- [9] Gatti A M, Valdrè G and Tombesi A 1996 *J. Biomed. Mater. Res.* **31** 475
- [10] Small J A 2002 *J. Res. Natl. Inst. Stand. Technol.* **107** 555
- [11] Paoletti L, Bruni B M, Gianfagna A, Mazziotti-Tagliani S and Pacella A 2011 *Microsc. Microanal.* **17** 710
- [12] Paoletti L, Bruni B M, Arrizza L, Mazziotti-Tagliani S and Pacella A 2008 *Per. Mineral.* **77** 63
- [13] Merlet C and Llovet X 2012 *IOP Conf. Series: Mater. Sci. Engng.* **32** 012016
- [14] Merlet C and Llovet X 2011 *X-ray Spectrom.* **40** 47
- [15] Salvat F, Llovet X, Fernández-Varea J M and Sempau J 2006 *Microchim. Acta* **155** 67
- [16] Ritchie N W M 2005 *Surf. Interface Anal.* **37** 1006
- [17] Skinner H C W 2003 *Indoor Built Environ.* **12** 385
- [18] Wiewióra A 1990 *Clay Min.* **25** 93

- [19] Hawthorne F C and Oberti R 2007 Amphiboles: crystal chemistry. in: *Amphiboles: Crystal Chemistry, Occurrence, and Health Issues. (Reviews in Mineralogy & Geochemistry vol 67)* (Hawthorne F C, Oberti R, Della Ventura G and Mottana A; Eds.) (Chantilly, VA: Mineralogical Society of America) chapter 1 pp 1-54
- [20] Hawthorne F C and Oberti R 2007 Classification of the amphiboles. in: *Amphiboles: Crystal Chemistry, Occurrence, and Health Issues (Reviews in Mineralogy & Geochemistry vol. 67)* (Hawthorne F C, Oberti R, Della Ventura G and Mottana A; Eds.) (Chantilly, VA: Mineralogical Society of America) chapter 2 pp 55-88
- [21] Hawthorne F C, Oberti R, Harlow G E, Maresch W V, Martin R F, Schumacher J C and Welch M D 2012 *Am. Mineralogist* **97** 2031
- [22] Czyzewski Z, MacCalum D O'N, Romig A and Joy D C 1990 *J. Appl. Phys.* **68** 3066
- [23] Jablonski A, Salvat F and Powell C J 2010 *NIST electron elastic-scattering cross-section database*. (Gaithersburg, MD: National Institute of Standards and Technology)
- [24] Joy D C and Luo S 1989 *Scanning* **11** 176
- [25] Bethe H A and Ashkin J 1953 Passage of radiations through matter. in: *Experimental Nuclear Physics* vol 1. (Segré E; Ed.) (New York, NY: Wiley)
- [26] Casnati E, Tartari A and Baraldi C 1982 *J. Phys. B: At. Mol. Opt. Phys.* **15** 155
- [27] Heinrich K F J 1986 in: *Proc. 11th Int. Congr. of X-ray Optics and Microanalysis (London, Canada)* (Brown J D and Packwood R H; Eds.) (Ontario: University of Western Ontario) p 67
- [28] Bambynek W *et al.* 1972 *Rev. Mod. Phys.* **44** 716
- [29] Ritchie N W M 2010 *Microsc. Microanal.* **16** 248